Supporting Information

Operando Raman Spectroscopy of Amorphous Molybdenum Sulfide (MoS_x) during the Electrochemical Hydrogen Evolution Reaction: Identification of Sulfur Atoms as Catalytically Active Sites for H^+ Reduction

Yilin Deng,[†] Louisa Rui Lin Ting,[†,‡] Perlin Hui Lin Neo,[†] Yin-Jia Zhang,[§]

Andrew A Peterson[‖] and Boon Siang Yeo*[,†,‡]

[†]Department of Chemistry, Faculty of Science, National University of Singapore, 3 Science Drive 3, Singapore 117543

[‡]Solar Energy Research Institute of Singapore, National University of Singapore, 7 Engineering Drive 1, Singapore 117574.

[§]Department of Chemistry, Brown University, 324 Brook Street, Providence, Rhode Island 02912, United States

[‖]School of Engineering, Brown University, 184 Hope Street, Providence, Rhode Island 02912, United States

*Author to whom correspondence should be addressed to: chmyeos@nus.edu.sg, Fax: +65 6779 1691, Tel: +65 6516 2836

S1. Curve fitting parameters, assignment and quantification of XPS signals of MoS_x-AE and MoS_x-CE catalysts

All the XPS peak assignments are summarized in Table S1. The Mo 3d spectra were fitted using a 3.2 eV separation between the $3d_{5/2}$ and $3d_{3/2}$ signals. The ratio of their peak areas was 3:2. The full width at half maximum (FWHM) for each pair of Mo 3d peaks was kept constant.[1] For the S 2p spectra, the peak separation was 1.2 eV between the $2p_{3/2}$ and $2p_{1/2}$ signals. The ratio of their peak areas was 2:1. The full width at half maximum (FWHM) for each pair of S 2p peaks was kept constant.[1]

By normalizing the signals against their specific relative sensitivity factors (RSF), the ratios of Mo: S could be derived from their relative peak areas. For example, in MoS_x-AE, the areas of the Mo 3d and S 2p peaks were 23722 and 14970 A.U. The relative sensitivity factors (RSF) for Mo 3d and S 2p are 3.321 and 0.668, respectively.

Hence, in MoS_x-AE the ratio of Mo: S atoms = $\frac{23722}{3.321}:\frac{14970}{0.668} = 1:3.1$

The ratios of S atoms with high and low electron binding energies could also be similarly derived. The S 2p peak could be further deconvoluted into low electron binding energy S and high electron binding energy S peaks, with the areas of 7275 and 7695 respectively. The ratio of low electron binding energy S: high electron binding energy S atoms = $\frac{7275}{0.668}:\frac{7695}{0.668} = 49:51$.

Table S1: Assignment of XPS Signals of MoS_x-AE and MoS_x-CE

Signal	Binding Energies (eV)	Assignment	References
Mo^{IV}	229.8 ($3d_{5/2}$), 233.0 ($3d_{3/2}$)	Mo centre of Mo-S catalysts	2-4
Mo^{VI}	232.4 ($3d_{5/2}$), 235.6 ($3d_{3/2}$)	MoO_3	2,5
S atoms with lower BE	162.5 ($2p_{3/2}$), 163.7 ($2p_{1/2}$)	Unsaturated S^{2-} in amorphous MoS_x Terminal S_2^{2-} in amorphous MoS_x	2,6-8
S atoms with higher BE	163.8 ($2p_{3/2}$), 165.0 ($2p_{1/2}$)	Apical S^{2-} in amorphous MoS_x Bridging S_2^{2-} in amorphous MoS_x	2,4,6,8

S2. Electrochemical/Raman Setup

The schematic diagram of the electrochemical/Raman spectroscopy setup is shown in Figure S1.

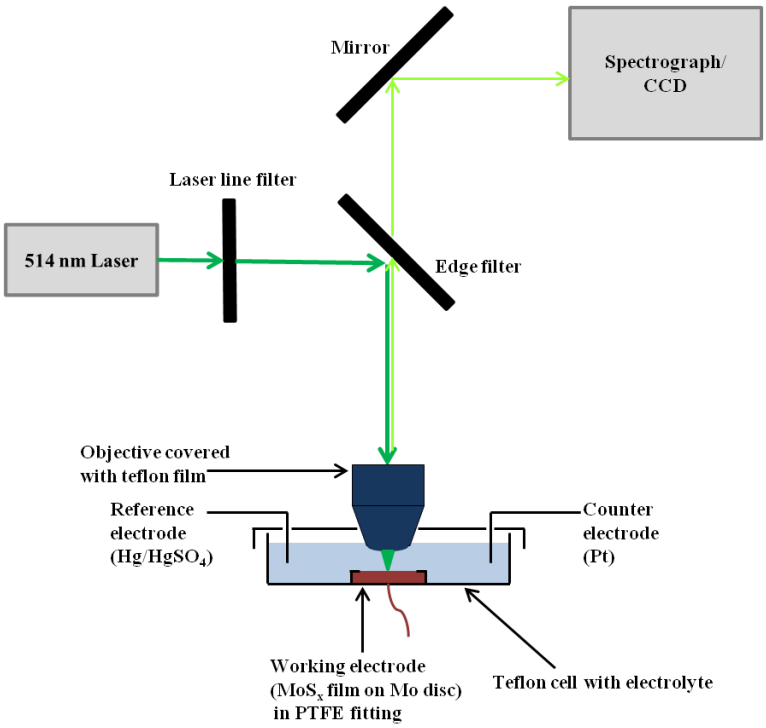

Figure S1: Schematic diagram of the electrochemical/Raman spectroscopy setup.

Each spectrum presented in this work is an average of three continuously acquired spectra with a collection time of 10 s each, except for that of the MoS_x-AE sample at 0.40 V, 0.28 V and 0.18 V (all potentials are vs. RHE) during the cathodic sweep of CV, which are an average of 9 spectra with a collection time of 10 s each. The Raman spectrum of crystalline MoS_2 (99%, Sigma Aldrich) is an average of 16 continuously acquired spectra with collection time of 5 s each.

S3. Atom % D in deuterated electrolyte (1 M $DClO_4$)

The 1 M $DClO_4$ was prepared from 8.625 mL of $HClO_4$ (70%, Sigma Aldrich) and 91.38 mL of D_2O (99.9 atom % D, Cambridge Isotope).

Densities of the 70% $HClO_4$ and the commercial D_2O at 25 ^oC are 1.664 g/mL and 1.107 g/mL respectively.

Molar mass:

$M(HClO_4) = 1.01 + 35.45 + 16.00 \times 4 = 100.46$ g/mol

$M(H_2O) = 1.01 \times 2 + 16.00 = 18.02$ g/mol.

$M(D_2O) = 2.01 \times 2 + 16.00 = 20.02$ g/mol.

In 8.625 mL of 70% $HClO_4$, the number of moles of $HClO_4$ and H_2O are:

Number of moles of $HClO_4$ $= \frac{m(HClO_4)}{M(HClO_4)} = \frac{8.625\text{mL}\times1.664\text{ g/mL}\times70\%}{100.46\text{ g/mol}} = 0.10$ mol

Number of moles of H_2O $= \frac{m(H_2O)}{M(H_2O)} = \frac{8.625\text{mL}\times1.664\text{ g/mL}\times30\%}{18.02\text{ g/mol}} = 0.24$ mol

Therefore, the total number of moles of H from 70% $HClO_4$:

$= 0.10 \text{ mol} + 0.24 \times 2 \text{ mol} = 0.58$ mol

The number of moles of both H and D from the commercial D_2O:

$$= \frac{m(D_2O)}{M(H_2O)\times0.1\%+M(D_2O)\times99.9\%} \times 2 = \frac{91.38\text{ mL}\times1.107\text{ g/mL}}{18.02\text{ g/mol}\times0.1\%+20.02\text{ g/mol}\times99.9\%} \times 2 = 10.11 \text{ mol}$$

The number of moles of H from the commercial D_2O:

$= 10.11 \text{ mol} \times 0.1\% = 0.01$ mol

Hence, the atom % H in the 1 M $DClO_4$:

$$= \frac{\text{Total number of moles of H}}{\text{Total number of moles of both H and D}} = \frac{0.58\text{mol}+0.01\text{ mol}}{0.58\text{mol}+10.11\text{ mol}} = 5.5\%$$

Therefore, the atom % D is:

100% - 5.5% = 94.5%

S4. Calculation of turnover frequencies

S4.1. Determination of the number of active sites in MoS_x-AE and MoS_x-CE using oxidative stripping

Cyclic voltammetry stripping was performed to oxidize the deposited films (Figure S2).[9] The HER performances of both samples were negligible after oxidative stripping to 1.3 V vs. RHE. This indicates that the active sites of the deposited films have been removed. Hence, the integrated charges beneath the oxidative peaks represent the amount of active sites in the films.[9,10]

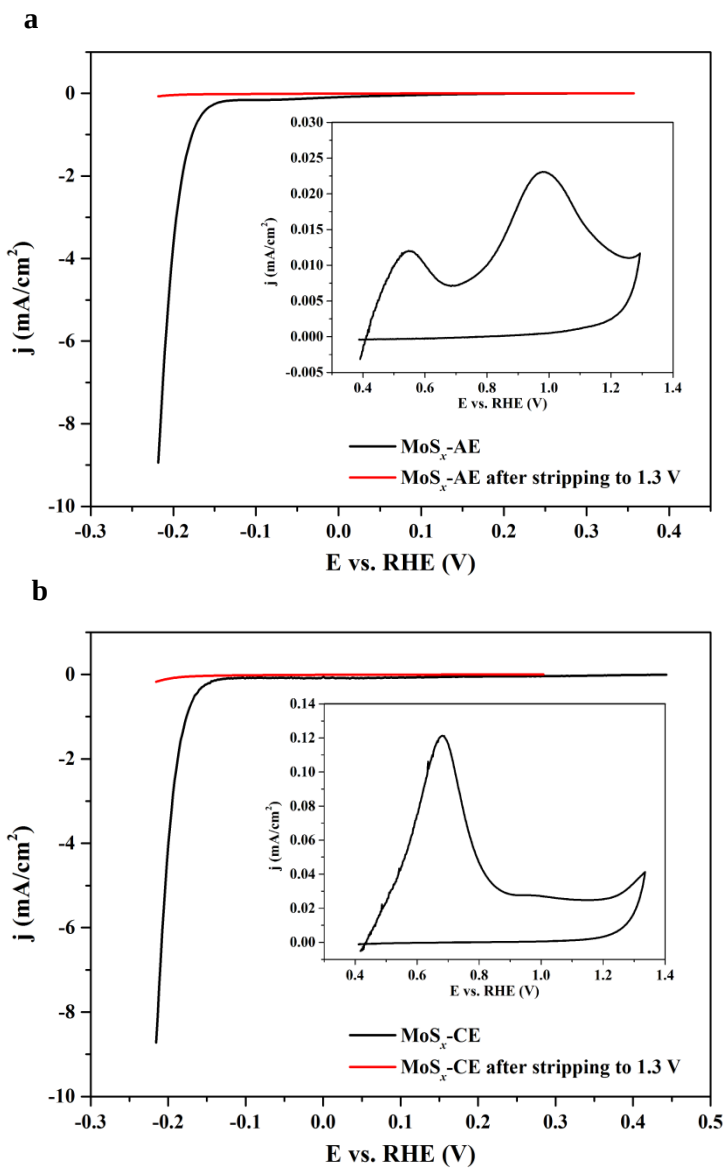

Figure S2: Linear sweep voltammograms of (a) MoS_x-AE and (b) MoS_x-CE before and after CV stripping to 1.3 V vs RHE in 1 M $HClO_4$. Insets show the corresponding CV stripping curves. Scan rate: 2 mV/s.

S4.2. Calculation of turnover frequencies

Using one measurement of MoS_x-AE catalyst as an example:

The turnover frequency (TOF) is expressed as:

$$TOF = \frac{Number\ of\ H_2\ molecules\ evolved\ per\ second}{Number\ of\ Active\ Sites}$$

Number of H_2 molecules evolved per second (assuming 100% Faradic efficiency in the HER process)[9]:

$$= \frac{i}{96485\ C\ per\ mole\ e^-} \times \frac{6.023\times10^{23}\ e^-\ per\ mole}{2\ e^-\ per\ molecule\ of\ H_2}$$

(where i is the current in amperes).

At an overpotential of 200mV, observed HER current in Figure S2a is $i = 1.51 \times 10^{-3}$ A.

The number of active sites, in this case, is determined by integrating the charge beneath the oxidative peaks in the anodic stripping CV, assuming a one-electron transfer process for the oxidation.[10]

$$Number\ of\ active\ sites = \frac{Q_{CV}}{96485\ C\ per\ mole\ e^-} \times \frac{6.023\times10^{23}\ e^-\ per\ mole}{1\ e^-\ per\ active\ site\ oxidised}$$

$$\text{Charge passed} = Q_{CV} = \int i_{CV}\, dt = 2.98 \times 10^{-3}\ \text{C}$$

Hence,

$$TOF = \frac{\left(\frac{i}{96485\ C\ per\ mole\ e^-} \times \frac{6.023\times10^{23}\ e^-\ per\ mole}{2\ e^-\ per\ molecule\ of\ H_2}\right)}{\left(\frac{Q_{CV}}{96485\ C\ per\ mole\ e^-} \times \frac{6.023\times10^{23}\ e^-\ per\ mole}{1\ e^-\ per\ active\ site\ oxidised}\right)} = \frac{i}{2Q_{CV}} = \frac{1.51\times10^{-3}}{2\times2.98\times10^{-3}} = 0.25\ \text{s}^{-1}$$

The TOFs of H_2 evolution exhibited by MoS_x-AE and MoS_x-CE were an average of three measurements of each catalyst (Section 3.2).

S5. Cyclic voltammograms of MoS_x-AE and MoS_x-CE with graphite counter electrode

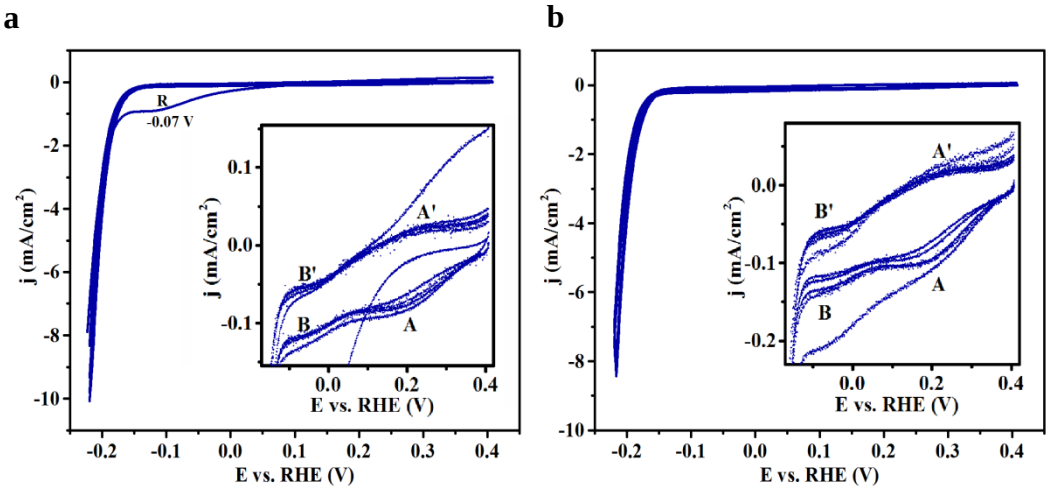

Figure S3: Cyclic voltammograms (cathodic sweep first) of (a) MoS_x-AE and (b) MoS_x-CE catalysts in 1 M $HClO_4$ electrolyte. Insets show a zoomed-in of the same curves. A graphite rod in lieu of a Pt counter electrode was used. Scan rate: 10 mV/s.

S6. Cyclic voltammograms of MoS_x-AE and MoS_x-CE at 0.5 mV/s during operando Raman spectroscopy measurements

Cyclic voltammograms of MoS_x-AE and MoS_x-CE were recorded at scan rates of 0.5 mV/s while operando Raman spectra were collected. Tafel slope values shown in the insets of Figures 2a(iii) and 2b(iii) were obtained from these CVs.

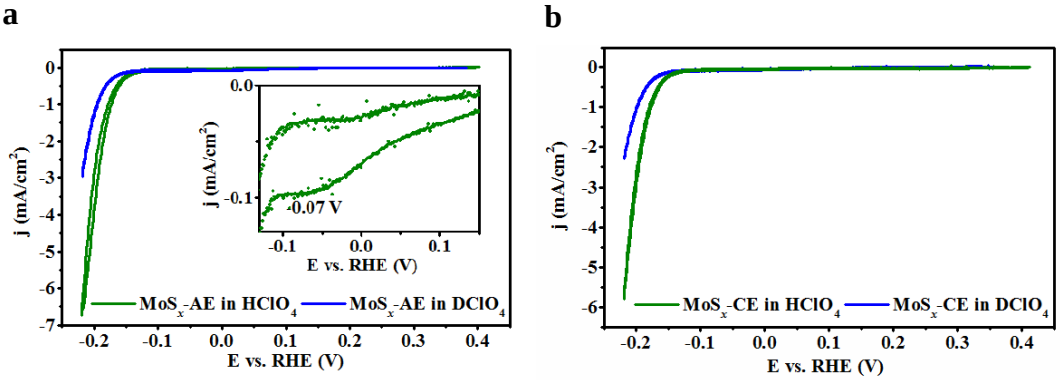

Figure S4: Cyclic voltammograms (cathodic sweep first) of (a) MoS_x-AE and (b) MoS_x-CE catalysts in 1 M $HClO_4$ and 1 M $DClO_4$ (containing 94.5 atom % D) electrolytes (the inset shows a zoomed-in of the MoS_x-AE reduction peak from the same curve). Scan rate: 0.5 mV/s.

S7. Raman spectra of electrodeposited MoS_x-AE, MoS_x-CE and crystalline MoS_2 in air

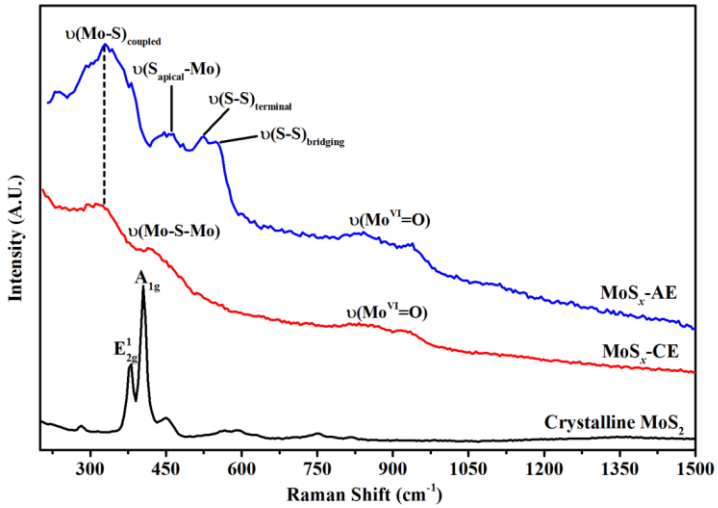

Figure S5: Raman spectra of crystalline MoS_2 (black curve), MoS_x-CE (red curve) and MoS_x-AE (blue curve) in air. MoS_x-CE and MoS_x-AE do not show the characteristic peaks of crystalline MoS_2.[11,12]

S8. Operando Raman spectra of MoS_x-AE and MoS_x-CE in 1M $DClO_4$ (94.5 atom % D)

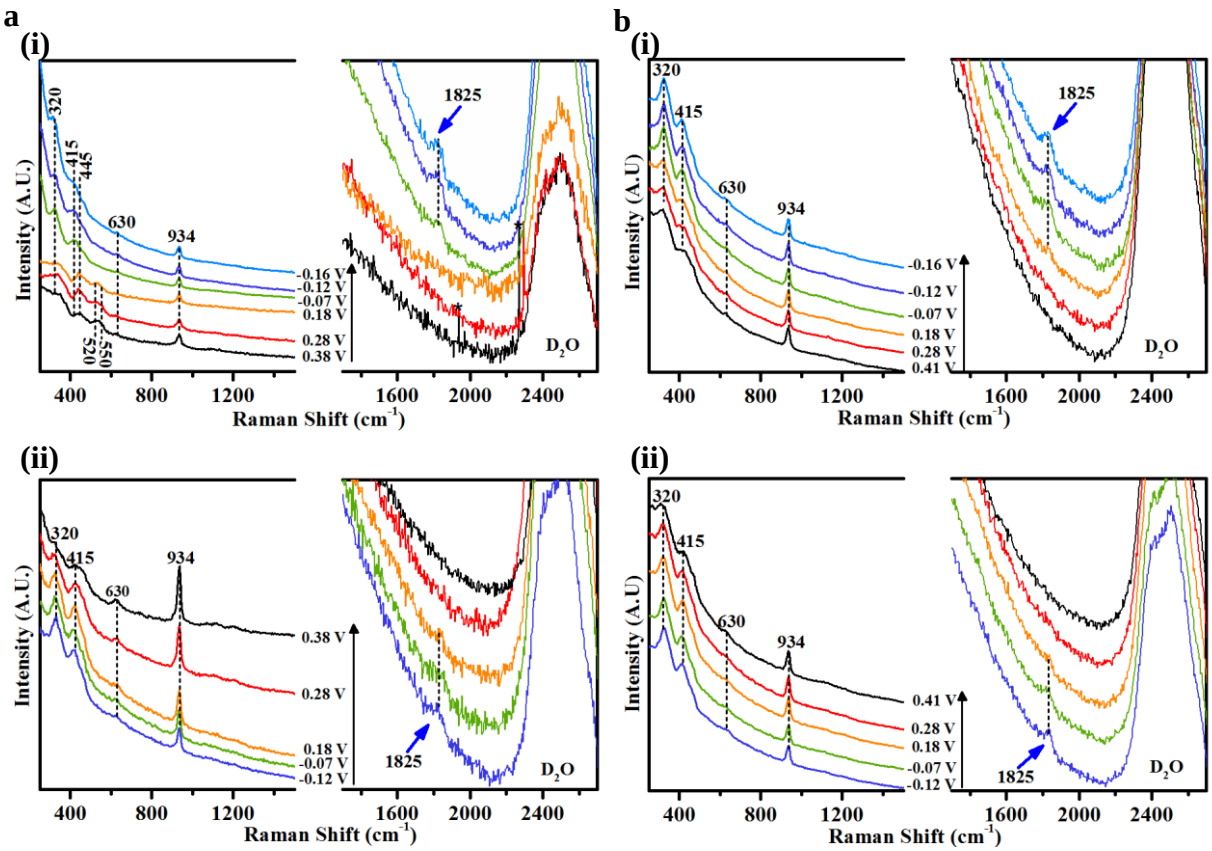

Figure S6: Raman spectra recorded from (a) MoS_x-AE and (b) MoS_x-CE catalysts during the (i) cathodic half sweep, and (ii) anodic half sweep of the cyclic voltammetry in 1 M $DClO_4$ (shown in section S6 of the Supporting Information, Figure S4). The signals marked with an asterisk originated from a cosmic ray.

S9. Operando Raman spectroscopy of Mo substrate in 1 M $HClO_4$

S9.1. Cyclic voltammogram of Mo substrate in 1 M $HClO_4$ at 0.5 mV/s

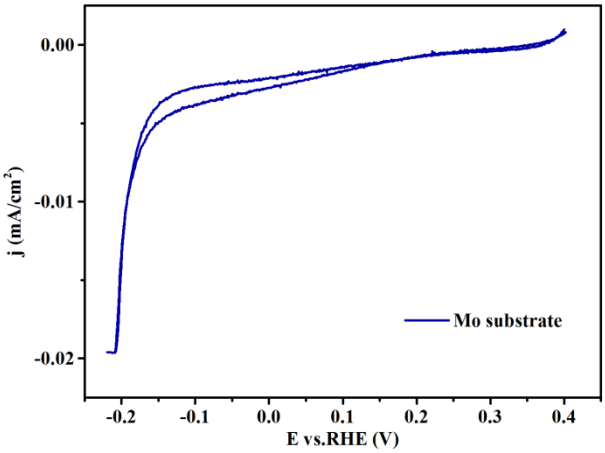

Figure S7: Cyclic voltammogram of Mo disc substrate in 1 M $HClO_4$. Scan rate: 0.5 mV/s.

S9.2. Raman spectra of Mo substrate collected during CV in 1 M $HClO_4$

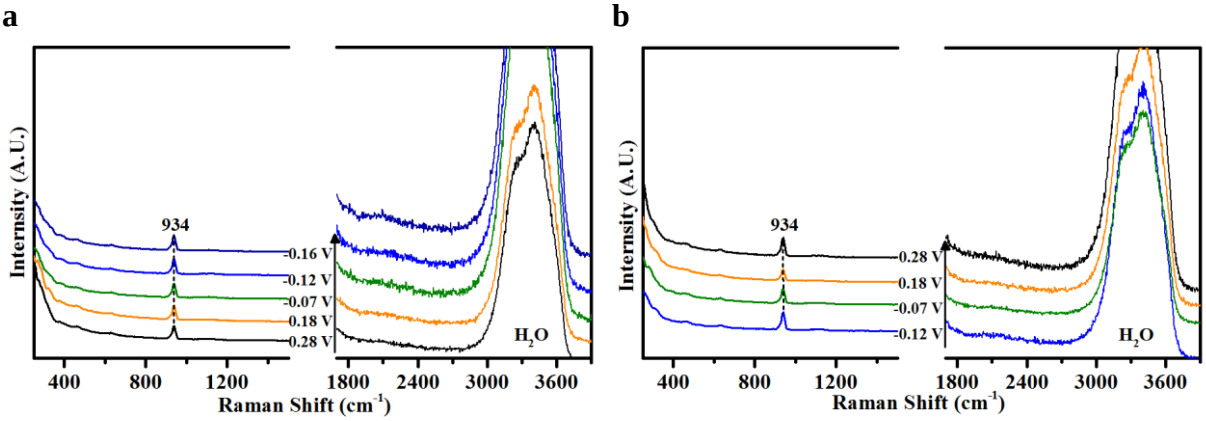

Figure S8: Sequence of Raman spectra recorded from bare Mo substrate during the (a) cathodic half sweep, and (b) anodic half sweep of the cyclic voltammetry in 1 M $HClO_4$ (shown in Figure S7). The Raman peaks at 934 and 3000-3600 cm^{-1} are vibrations of ClO_4^- and H_2O, respectively.[13] The 2530 cm^{-1} peak, attributed to ν(S-H), is absent.

References

(1) Moulder, J. F.; Stickle, W. F.; Sobol, P. E.; Bomben, K. D. *Handbook of X-ray Photoelectron Spectroscopy*; Physical Electronics Inc.: Eden Prairie, MN, U.S.A., 1995.

(2) Muijsers, J. C.; Weber, T.; van Hardeveld, R. M.; Zandbergen, H. W.; Niemantsverdriet, J. W. *J. Catal.* **1995**, 157, 698-705.

(3) Wang, T. Y.; Gao, D. L.; Zhuo, J. Q.; Zhu, Z. W.; Papakonstantinou, P.; Li, Y.; Li, M. X. *Chem. - Eur. J.* **2013**, 19, 11939-11948.

(4) Muller, A.; Wittneben, V.; Krickemeyer, E.; Bogge, H.; Lemke, M. *Z. Anorg. Allg. Chem.* **1991**, 605, 175-188.

(5) Vrubel, H.; Hu, X. *ACS Catal.* **2013**, 3, 2002-2011.

(6) Kibsgaard, J.; Jaramillo, T. F.; Besenbacher, F. *Nat. Chem.* **2014**, 6, 248-253.

(7) Jaramillo, T. F.; Bonde, J.; Zhang, J.; Ooi, B.-L.; Andersson, K.; Ulstrup, J.; Chorkendorff, I. *J. Phys. Chem. C* **2008**, 112, 17492-17498.

(8) Hou, Y.; Abrams, B. L.; Vesborg, P. C. K.; Björketun, M. E.; Herbst, K.; Bech, L.; Setti, A. M.; Damsgaard, C. D.; Pedersen, T.; Hansen, O.; Rossmeisl, J.; Dahl, S.; Nørskov, J. K.; Chorkendorff, I. *Nat. Mater.* **2011**, 10, 434-438.

(9) Ting, L. R. L.; Deng, Y.; Ma, L.; Zhang, Y.-J.; Peterson, A. A.; Yeo, B. S. *ACS Catal.* **2016**, 6, 861-867.

(10) Merki, D.; Fierro, S.; Vrubel, H.; Hu, X. L. *Chem. Sci.* **2011**, 2, 1262-1267.

(11) Benck, J. D.; Chen, Z.; Kuritzky, L. Y.; Forman, A. J.; Jaramillo, T. F. *ACS Catal.* **2012**, 2, 1916-1923.

(12) Voiry, D.; Salehi, M.; Silva, R.; Fujita, T.; Chen, M.; Asefa, T.; Shenoy, V. B.; Eda, G.; Chhowalla, M. *Nano Lett.* **2013**, 13, 6222-6227.

(13) Ratcliffe, C.; Irish, D. *Can. J. Chem.* **1984**, 62, 1134-1144.